



Fermi National Accelerator Laboratory

FERMILAB Pub-94/208-E
CDF

A Precision Measurement of the Prompt Photon Cross Section in $p\bar{p}$ Collisions at $\sqrt{s} = 1.8$ TeV

The CDF Collaboration

*Fermi National Accelerator Laboratory
P.O. Box 500, Batavia, Illinois 60510*

July 1994

Submitted to Physical Review Letters.

Disclaimer

This report was prepared as an account of work sponsored by an agency of the United States Government. Neither the United States Government nor any agency thereof, nor any of their employees, makes any warranty, express or implied, or assumes any legal liability or responsibility for the accuracy, completeness, or usefulness of any information, apparatus, product, or process disclosed, or represents that its use would not infringe privately owned rights. Reference herein to any specific commercial product, process, or service by trade name, trademark, manufacturer, or otherwise, does not necessarily constitute or imply its endorsement, recommendation, or favoring by the United States Government or any agency thereof. The views and opinions of authors expressed herein do not necessarily state or reflect those of the United States Government or any agency thereof.

A Precision Measurement of the Prompt Photon Cross Section in $p\bar{p}$ Collisions at $\sqrt{s} = 1.8$ TeV

F. Abe,¹³ M. G. Albrow,⁷ D. Amidei,¹⁶ J. Antos,²⁸ C. Anway-Wiese,⁴ G. Apollinari,²⁶
H. Areti,⁷ M. Atac,⁷ P. Auchincloss,²⁵ F. Azfar,²¹ P. Azzi,²⁰ N. Bacchetta,¹⁸ W. Badgett,¹⁶
M. W. Bailey,¹⁸ J. Bao,³⁴ P. de Barbaro,²⁵ A. Barbaro-Galtieri,¹⁴ V. E. Barnes,²⁴
B. A. Barnett,¹² P. Bartalini,²³ G. Bauer,¹⁵ T. Baumann,⁹ F. Bedeschi,²³ S. Behrends,³
S. Belforte,²³ G. Bellettini,²³ J. Bellinger,³³ D. Benjamin,³² J. Benloch,¹⁵ J. Bensinger,³
D. Benton,²¹ A. Beretvas,⁷ J. P. Berge,⁷ S. Bertolucci,⁸ A. Bhatti,²⁶ K. Biery,¹¹ M. Binkley,⁷
F. Bird,²⁹ D. Bisello,²⁰ R. E. Blair,¹ C. Blocker,²⁹ A. Bodek,²⁵ W. Bokhari,¹⁵ V. Bolognesi,²³
D. Bortoletto,²⁴ C. Boswell,¹² T. Boulos,¹⁴ G. Brandenburg,⁹ E. Buckley-Geer,⁷ H. S. Budd,²⁵
K. Burkett,¹⁶ G. Busetto,²⁰ A. Byon-Wagner,⁷ K. L. Byrum,¹ J. Cammerata,¹²
C. Campagnari,⁷ M. Campbell,¹⁶ A. Caner,⁷ W. Carithers,¹⁴ D. Carlsmith,³³ A. Castro,²⁰
Y. Cen,²¹ F. Cervelli,²³ J. Chapman,¹⁶ M.-T. Cheng,²⁸ G. Chiarelli,⁸ T. Chikamatsu,³¹
S. Cihangir,⁷ A. G. Clark,²³ M. Cobal,²³ M. Contreras,⁵ J. Conway,²⁷ J. Cooper,⁷
M. Cordelli,⁸ D. Crane,¹ J. D. Cunningham,³ T. Daniels,¹⁵ F. DeJongh,⁷ S. Delchamps,⁷
S. Dell'Agnello,²³ M. Dell'Orso,²³ L. Demortier,²⁶ B. Denby,²³ M. Deninno,² P. F. Derwent,¹⁶
T. Devlin,²⁷ M. Dickson,²⁵ S. Donati,²³ R. B. Drucker,¹⁴ A. Dunn,¹⁶ K. Einsweiler,¹⁴
J. E. Elias,⁷ R. Ely,¹⁴ E. Engels, Jr.,²² S. Eno,⁵ D. Errede,¹⁰ S. Errede,¹⁰ Q. Fan,²⁵

Submitted to Phys. Rev. Lett. July 25, 1994

B. Farhat,¹⁵ I. Fiori,² B. Flaughner,⁷ G. W. Foster,⁷ M. Franklin,⁹ M. Frautschi,¹⁸ J. Freeman,⁷
J. Friedman,¹⁵ H. Frisch,⁵ A. Fry,²⁹ T. A. Fuess,¹ Y. Fukui,¹³ S. Funaki,³¹ G. Gagliardi,²³
S. Galeotti,²³ M. Gallinaro,²⁰ A. F. Garfinkel,²⁴ S. Geer,⁷ D. W. Gerdes,¹⁶ P. Giannetti,²³
N. Giokaris,²⁶ P. Giromini,⁸ L. Gladney,²¹ D. Glenzinski,¹² M. Gold,¹⁸ J. Gonzalez,²¹
A. Gordon,⁹ A. T. Goshaw,⁶ K. Goulianos,²⁶ H. Grassmann,⁶ A. Grewal,²¹ G. Grieco,²³
L. Groer,²⁷ C. Grosso-Pilcher,⁵ C. Haber,¹⁴ S. R. Hahn,⁷ R. Hamilton,⁹ R. Handler,³³
R. M. Hans,³⁴ K. Hara,³¹ B. Harral,²¹ R. M. Harris,⁷ S. A. Hauger,⁶ J. Hauser,⁴ C. Hawk,²⁷
J. Heinrich,²¹ D. Cronin-Hennessy,⁶ R. Hollebeek,²¹ L. Holloway,¹⁰ A. Hölscher,¹¹ S. Hong,¹⁶
G. Houk,²¹ P. Hu,²² B. T. Huffman,²² R. Hughes,²⁵ P. Hurst,⁹ J. Huston,¹⁷ J. Huth,⁹
J. Hysten,⁷ M. Incagli,²³ J. Incandela,⁷ H. Iso,³¹ H. Jensen,⁷ C. P. Jessop,⁹ U. Joshi,⁷
R. W. Kadel,¹⁴ E. Kajfasz,^{7a} T. Kamon,³⁰ T. Kaneko,³¹ D. A. Kardelis,¹⁰ H. Kasha,³⁴
Y. Kato,¹⁹ L. Keeble,³⁰ R. D. Kennedy,²⁷ R. Kephart,⁷ P. Kesten,¹⁴ D. Kestenbaum,⁹
R. M. Keup,¹⁰ H. Keutelian,⁷ F. Keyvan,⁴ D. H. Kim,⁷ H. S. Kim,¹¹ S. B. Kim,¹⁶ S. H. Kim,³¹
Y. K. Kim,¹⁴ L. Kirsch,³ P. Koehn,²⁵ K. Kondo,³¹ J. Konigsberg,⁹ S. Kopp,⁵ K. Kordas,¹¹
W. Koska,⁷ E. Kovacs,^{7a} W. Kowald,⁶ M. Krasberg,¹⁶ J. Kroll,⁷ M. Kruse,²⁴ S. E. Kuhlmann,¹
E. Kuns,²⁷ A. T. Laasanen,²⁴ S. Lammel,⁴ J. I. Lamoureux,³ T. LeCompte,¹⁰ S. Leone,²³
J. D. Lewis,⁷ P. Limon,⁷ M. Lindgren,⁴ T. M. Liss,¹⁰ N. Lockyer,²¹ C. Loomis,²⁷
O. Long,²¹ M. Loreti,²⁰ E. H. Low,²¹ J. Lu,³⁰ D. Lucchesi,²³ C. B. Luchini,¹⁰ P. Lukens,⁷
P. Maas,³³ K. Maeshima,⁷ A. Maghakian,²⁶ P. Maksimovic,¹⁵ M. Mangano,²³ J. Mansour,¹⁷
M. Mariotti,²³ J. P. Marriner,⁷ A. Martin,¹⁰ J. A. J. Matthews,¹⁸ R. Mattingly,¹⁵
P. McIntyre,³⁰ P. Melese,²⁶ A. Menzione,²³ E. Meschi,²³ G. Michail,⁹ S. Mikamo,¹³ M. Miller,⁵

R. Miller,¹⁷ T. Mimashi,³¹ S. Miscetti,⁸ M. Mishina,¹³ H. Mitsushio,³¹ S. Miyashita,³¹
Y. Morita,¹³ S. Moulding,²⁶ J. Mueller,²⁷ A. Mukherjee,⁷ T. Muller,⁴ P. Musgrave,¹¹
L. F. Nakae,²⁹ I. Nakano,³¹ C. Nelson,⁷ D. Neuberger,⁴ C. Newman-Holmes,⁷ L. Nodulman,¹
S. Ogawa,³¹ S. H. Oh,⁶ K. E. Ohl,³⁴ R. Oishi,³¹ T. Okusawa,¹⁹ C. Pagliarone,²³
R. Paoletti,²³ V. Papadimitriou,⁷ S. Park,⁷ J. Patrick,⁷ G. Pauletta,²³ M. Paulini,¹⁴
L. Pescara,²⁰ M. D. Peters,¹⁴ T. J. Phillips,⁶ G. Piacentino,² M. Pillai,²⁵ R. Plunkett,⁷
L. Pondrom,³³ N. Product,¹⁴ J. Proudfoot,¹ F. Ptohos,⁹ G. Punzi,²³ K. Ragan,¹¹ F. Rimondi,²
L. Ristori,²³ M. Roach-Bellino,³² W. J. Robertson,⁶ T. Rodrigo,⁷ J. Romano,⁵ L. Rosenson,¹⁵
W. K. Sakumoto,²⁵ D. Saltzberg,⁵ A. Sansoni,⁸ V. Scarpine,³⁰ A. Schindler,¹⁴ P. Schlabach,⁹
E. E. Schmidt,⁷ M. P. Schmidt,³⁴ O. Schneider,¹⁴ G. F. Sciacca,²³ A. Scribano,²³ S. Segler,⁷
S. Seidel,¹⁸ Y. Seiya,³¹ G. Sganos,¹¹ A. Sgolacchia,² M. Shapiro,¹⁴ N. M. Shaw,²⁴ Q. Shen,²⁴
P. F. Shepard,²² M. Shimojima,³¹ M. Shochet,⁵ J. Siegrist,²⁹ A. Sill,^{7a} P. Sinervo,¹¹ P. Singh,²²
J. Skarha,¹² K. Sliwa,³² D. A. Smith,²³ F. D. Snider,¹² L. Song,⁷ T. Song,¹⁶ J. Spalding,⁷
L. Spiegel,⁷ P. Sphicas,¹⁵ A. Spies,¹² L. Stanco,²⁰ J. Steele,³³ A. Stefanini,²³ K. Strahl,¹¹
J. Strait,⁷ D. Stuart,⁷ G. Sullivan,⁵ K. Sumorok,¹⁵ R. L. Swartz, Jr.,¹⁰ T. Takahashi,¹⁹
K. Takikawa,³¹ F. Tartarelli,²³ W. Taylor,¹¹ Y. Teramoto,¹⁹ S. Tether,¹⁵ D. Theriot,⁷
J. Thomas,²⁹ T. L. Thomas,¹⁸ R. Thun,¹⁶ M. Timko,³² P. Tipton,²⁵ A. Titov,²⁶ S. Tkaczyk,⁷
K. Tollefson,²⁵ A. Tollestrup,⁷ J. Tonnison,²⁴ J. F. de Troconiz,⁹ J. Tseng,¹² M. Turcotte,²⁹
N. Turini,² N. Uemura,³¹ F. Ukegawa,²¹ G. Unal,²¹ S. van den Brink,²² S. Vejcik, III,¹⁶
R. Vidal,⁷ M. Vondracek,¹⁰ R. G. Wagner,¹ R. L. Wagner,⁷ N. Wainer,⁷ R. C. Walker,²⁵
G. Wang,²³ J. Wang,⁵ M. J. Wang,²⁸ Q. F. Wang,²⁶ A. Warburton,¹¹ G. Watts,²⁵ T. Watts,²⁷

R. Webb,³⁰ C. Wendt,³³ H. Wenzel,¹⁴ W. C. Wester, III,¹⁴ T. Westhusing,¹⁰ A. B. Wicklund,¹
E. Wicklund,⁷ R. Wilkinson,²¹ H. H. Williams,²¹ P. Wilson,⁵ B. L. Winer,²⁵ J. Wolinski,³⁰
D. Y. Wu,¹⁶ X. Wu,²³ J. Wyss,²⁰ A. Yagil,⁷ W. Yao,¹⁴ K. Yasuoka,³¹ Y. Ye,¹¹ G. P. Yeh,⁷
P. Yeh,²⁸ M. Yin,⁶ J. Yoh,⁷ T. Yoshida,¹⁹ D. Yovanovitch,⁷ I. Yu,³⁴ J. C. Yun,⁷ A. Zanetti,²³
F. Zetti,²³ L. Zhang,³³ S. Zhang,¹⁶ W. Zhang,²¹ and S. Zucchelli²

(CDF Collaboration)

¹ *Argonne National Laboratory, Argonne, Illinois 60439*

² *Istituto Nazionale di Fisica Nucleare, University of Bologna, I-40126 Bologna, Italy*

³ *Brandeis University, Waltham, Massachusetts 02254*

⁴ *University of California at Los Angeles, Los Angeles, California 90024*

⁵ *University of Chicago, Chicago, Illinois 60637*

⁶ *Duke University, Durham, North Carolina 27708*

⁷ *Fermi National Accelerator Laboratory, Batavia, Illinois 60510*

⁸ *Laboratori Nazionali di Frascati, Istituto Nazionale di Fisica Nucleare, I-00044 Frascati, Italy*

⁹ *Harvard University, Cambridge, Massachusetts 02138*

¹⁰ *University of Illinois, Urbana, Illinois 61801*

¹¹ *Institute of Particle Physics, McGill University, Montreal H3A 2T8, and University of Toronto,*

Toronto M5S 1A7, Canada

¹² *The Johns Hopkins University, Baltimore, Maryland 21218*

¹³ *National Laboratory for High Energy Physics (KEK), Tsukuba, Ibaraki 305, Japan*

- ¹⁴ *Lawrence Berkeley Laboratory, Berkeley, California 94720*
- ¹⁵ *Massachusetts Institute of Technology, Cambridge, Massachusetts 02139*
- ¹⁶ *University of Michigan, Ann Arbor, Michigan 48109*
- ¹⁷ *Michigan State University, East Lansing, Michigan 48824*
- ¹⁸ *University of New Mexico, Albuquerque, New Mexico 87131*
- ¹⁹ *Osaka City University, Osaka 588, Japan*
- ²⁰ *Universita di Padova, Istituto Nazionale di Fisica Nucleare, Sezione di Padova, I-35131 Padova, Italy*
- ²¹ *University of Pennsylvania, Philadelphia, Pennsylvania 19104*
- ²² *University of Pittsburgh, Pittsburgh, Pennsylvania 15260*
- ²³ *Istituto Nazionale di Fisica Nucleare, University and Scuola Normale Superiore of Pisa, I-56100 Pisa, Italy*
- ²⁴ *Purdue University, West Lafayette, Indiana 47907*
- ²⁵ *University of Rochester, Rochester, New York 14627*
- ²⁶ *Rockefeller University, New York, New York 10021*
- ²⁷ *Rutgers University, Piscataway, New Jersey 08854*
- ²⁸ *Academia Sinica, Taiwan 11529, Republic of China*
- ²⁹ *Superconducting Super Collider Laboratory, Dallas, Texas 75237*
- ³⁰ *Texas A&M University, College Station, Texas 77843*
- ³¹ *University of Tsukuba, Tsukuba, Ibaraki 305, Japan*
- ³² *Tufts University, Medford, Massachusetts 02155*
- ³³ *University of Wisconsin, Madison, Wisconsin 53706*
- ³⁴ *Yale University, New Haven, Connecticut 06511*

Abstract

A prompt photon cross section measurement from the CDF experiment at the Fermilab $p\bar{p}$ Collider is presented. Detector and trigger upgrades, as well as six times the integrated luminosity compared with our previous publication, have contributed to a much more precise measurement and extended P_T range. As before, QCD calculations agree qualitatively with the measured cross section but the data has a steeper slope than the calculations.

PACS number(s): 13.85.Qk, 12.38.Qk

In this letter we present a measurement of the cross section for production of isolated prompt photons in proton-antiproton collisions at $\sqrt{s} = 1.8$ TeV from the Collider Detector at Fermilab (CDF). Prompt photons are produced in the initial collision, in contrast to photons produced by decays of hadrons. In Quantum Chromodynamics (QCD), at lowest order, prompt photon production is dominated by the Compton process ($gq \rightarrow \gamma q$), which is sensitive to the gluon distribution of the proton [1]. With six times the direct photon sample coming from the 1992-1993 data, plus detector and trigger additions, the present measurement is a significant improvement over our previously published results [2]. The resulting statistical and systematic uncertainties are also significantly smaller than previous collider and fixed target experiments. The precision of the present measurement provides a quantitative test of QCD and parton distributions in a fractional momentum range $0.013 < x < 0.13$.

A detailed description of the CDF detector may be found in [3], and the important components are the same as used in the previous analysis [2], with one addition. In order to improve the measurement systematic uncertainties, and separate signal from background at higher photon P_T , a set of multiwire proportional chambers was added in front of the central electromagnetic calorimeter (CEM). These are called the Central Preshower (CPR) chambers, and they sample the electromagnetic showers that begin in the solenoid magnet material ($1.075 X_0$) in front of them. The chambers have 2.22 cm cells segmented in $r - \phi$, and are positioned at a radius of 168 cm from the beamline. There are 4 chamber divisions spanning ± 1.1 unit of pseudorapidity, η , (defined by the expression $\eta = -\ln(\tan \theta/2)$). The

other important detector component used for this analysis is the Central Electromagnetic Strip (CES) chamber system, used in the previously published measurement. These chambers, embedded at shower maximum, provide the photon position measurement as well as measuring the transverse profile of the electromagnetic shower.

In addition to the detector improvement noted above, the photon hardware trigger was upgraded. The photon trigger consists of three levels. At the first level, a single tower in the CEM is required to be above a threshold, typically $P_T > 6$ GeV/c. Previously in the second trigger level the only requirement was that 89% of the photon transverse energy be in the EM compartment of the calorimeter. Additional electronics were added at this level to require that the transverse energy in the 5×5 grid of trigger towers surrounding the photon candidate (equivalent to a radius $R = \sqrt{(\Delta\eta)^2 + (\Delta\phi)^2} = 0.65$) was less than 5 GeV, thereby requiring the photon to be *isolated*. With the upgraded trigger the threshold for the main photon trigger was 16 GeV/c, without it a prescaling of approximately $\times 100$ would have been needed for the 16-30 GeV/c P_T range, due to trigger rate limitations. In addition, a $P_T > 6$ GeV/c prescaled trigger with the same isolation requirement was used, as well as a $P_T > 50$ GeV/c trigger without the isolation cut. In the third level of the trigger, software algorithms applied fiducial cuts to the photons and stiffened the isolation cut to 4 GeV in a cone radius of 0.7. Integrated luminosities for the 3 trigger thresholds were 19, 16, 0.054 pb⁻¹ for the 50, 16, 6 GeV/c thresholds respectively, including the effect of prescales.

The selection of prompt photon candidates from the triggered events is essentially the same as those used previously [2], with some minor revisions. Candidates were rejected

if there was a reconstructed charged track pointing at the CPR chamber containing the photon. To improve the signal/background ratio, the isolation cut applied in the trigger was tightened to 2 GeV in a cone radius of 0.7. Cuts on the event z vertex and missing transverse energy were applied as before with slight changes [4]. At this point, the main backgrounds to the prompt photons are from single π^0 and η mesons, with smaller backgrounds from other multi- π^0 states. These backgrounds are all reduced by requiring there is no other photon candidate above 1 GeV energy in the CES. The total acceptance of prompt photons within $|\eta| < 0.9$, including efficiencies for all these cuts is approximately 38% with a small P_T dependence. This value is slightly smaller than our previously published acceptance due to the effect of multiple collisions at the higher luminosities.

We employ two methods for statistically subtracting the remaining neutral meson background from our photon candidates: the *conversion method* counts the fraction of photon conversions in the solenoid magnet material by using the CPR, and the *profile method* uses the transverse profile of the electromagnetic shower in the CES. For the conversion method, the probability of a single photon conversion is $\approx 60\%$, while that for the two-photon decay of a π^0 or η is larger, $\approx 84\%$. For the profile method, the transverse profile of each photon candidate was compared to that measured for electrons in a test beam in the same momentum range. A measure of the goodness of fit ($\tilde{\chi}^2$ [2]) was statistically larger for a neutral meson (poor fit) than for a single photon (good fit) because a neutral meson usually produced a wider EM shower. The conversion method has the advantage of much smaller systematic uncertainties and an unlimited P_T range. But the profile method has the advan-

tage of a better separation of signal and background than the conversion method in the low P_T region. We thus use the profile method from 10-16 GeV/c P_T and the conversion method everywhere else.

For both background subtraction methods, the number of photons (N_γ) in a bin of P_T is obtained from the number of photon candidates (N), the fraction of photon candidates that pass a fixed cut defined below (ϵ), and the corresponding fractions for true photons (ϵ_γ) and background (ϵ_b), using:

$$N_\gamma = \left(\frac{\epsilon - \epsilon_b}{\epsilon_\gamma - \epsilon_b} \right) N \quad (1)$$

Equation 1 comes from $\epsilon N = \epsilon_\gamma N_\gamma + \epsilon_b N_b$ with $N_b = N - N_\gamma$. For the conversion method, ϵ is the fraction of photon candidates which produce a pulse height of greater than 1 minimum ionizing particle in the CPR, within a 66 milliradian “window” (5 CPR channels) around the photon direction. For reference the minimum separation of the two photons from a 25 GeV/c π^0 is 11 mr. For the profile method, ϵ is the fraction of events which have $\tilde{\chi}^2 < 4$ out of all events with $\tilde{\chi}^2 < 20$. Using these methods, we measure the signal/background ratio bin-by-bin and propagate each bin’s statistical uncertainty into the cross section measurement, including the effect of the background subtraction.

For the conversion method ϵ_γ is estimated from the following equation:

$\epsilon_\gamma = 1 - \exp(-7/9 * t)$ where t is the amount of material in radiation lengths in front of the CPR. Corrections to this estimate of ϵ_γ are made on an event basis for the different amount of material traversed due to angular effects, as well as changes in the pair production cross section with photon energy [5]. An additional correction is made for photon showers that

begin after the photon has passed through the CPR, but a soft photon or electron from the shower is scattered backwards at a large angle and gives a CPR signal. This correction was estimated with an electromagnetic shower simulation [6]. The final correction to ϵ_γ , estimated using minimum bias triggers, is due to CPR signals arising from soft photons from the underlying event. The fraction of background events that give a CPR signal, ϵ_b , is the same as ϵ_γ except for the multiple photons from the background:

$\epsilon_b = 1 - \exp(-7/9 * t * N_\gamma(P_T))$. The function $N_\gamma(P_T)$ is the average number of photons within the CPR “window” defined earlier. This changes with particle P_T and type, and is estimated using a detector simulation of π^0 , η and K_S^0 mesons with a relative production ratio of 1:1:0.4 [2]. All of the corrections mentioned earlier for ϵ_γ are applied to ϵ_b as well.

For the profile method ϵ_γ and ϵ_b are the same as in reference [2]. For both methods ϵ , ϵ_γ , ϵ_b are shown in figure 1, along with ϵ for the previous measurement using only the profile method. Note that the data fractions are close to the single photon expectation at $P_T \geq 100$ GeV/c (signal/background ≈ 18), while they are consistent with nearly 100% background at $P_T < 10$ GeV/c. Due to this small signal/background ratio, cross section measurements will only be presented above 10 GeV/c at this time.

The systematic uncertainty in the prompt photon cross section is due mostly to uncertainties in ϵ_γ and ϵ_b . For both methods we can check these fractions using reconstructed π^0 , η , and ρ mesons, shown in figure 2. Reference [2] demonstrates how the signal and background regions were defined for the reconstructed peaks in the previous analysis, as well as the sideband subtractions. A similar technique is used in this analysis for the *measured* rates

in the CPR conversion method, and the *expected* rates were determined with the corrections to ϵ_γ and ϵ_b discussed earlier. The measured (expected) CPR conversion rate for the π^0 is $.842 \pm .008$ (.847), for the η is $.831 \pm .012$ (.842), and for the ρ is $.836 \pm .01$ (.834). The uncertainty in the expected CPR conversion rate, due to the material count for the solenoid magnet, is .006. There is excellent agreement between the measured and predicted rates in all three cases, thus we will use .006 for the uncertainty in ϵ_b . This translates into a .0078 uncertainty in ϵ_γ , and is completely correlated with the ϵ_b uncertainty. These uncertainties combined lead to a 7% uncertainty in the cross section measurement at 16 GeV/c P_T , and a 4.5% uncertainty at 100 GeV/c. The uncertainty in the cross section due to backscattered photons and electrons is 2% at 16 GeV/c and 7% at 100 GeV/c. The uncertainty in the η/π^0 ratio [2] leads to a cross section uncertainty of 2% at 16 GeV/c and 0.2% at 100 GeV/c. The entire mix of background sources has been checked by a sample of events with the same photon cuts as the data, but the isolation cut slightly relaxed. This shows agreement with expectations within the uncertainty on ϵ_b quoted above. Finally, there are additional uncertainties due to luminosity (3.6%), selection efficiencies (4.8%), and photon energy scale (4.5%). The uncertainties in the profile method are much larger (30-70%), and are given in [2], but the two methods agree to within 5% from 16-30 GeV/c.

From the number of prompt photons in a bin of transverse momentum, along with the acceptance and the integrated luminosity for that bin, we obtain the isolated prompt photon cross section which is tabulated in Table 1. The bin sizes were chosen to maintain sufficient statistics to perform the background subtraction. Also tabulated are the number of

events, number of photons after background subtraction, statistical and systematic uncertainties. The systematic uncertainties listed are approximately 100% correlated and include all normalization uncertainties.

In Fig. 3 our measurements from both 1989 and 1992 are compared to a next to leading order QCD calculation [7] derived using the CTEQ2M parton distributions [8] at a renormalization scale $\mu = P_T$. Inset is a comparison of the two background subtraction methods in their overlap region. The QCD prediction agrees qualitatively with the measurements over more than 4 orders of magnitude in cross section. Figure 4 shows the same on a linear scale, as well as the prediction using CTEQ2ML [8] and MRSD- [9] parton distributions. The QCD calculations shown do not reproduce the shape of the data, and many other variations of modern parton distributions and renormalization scale were attempted, with small ($\approx 5\%$) changes in the shape of the predictions. We note that while figure 4 gives the indication of an “excess” of photons at $P_T < 30$ GeV/c, that with a possible theory+experimental normalization shift upward of 20%, the “excess” changes to an overall shape difference. There are at least three possible explanations for this shape difference. Multiple soft gluon radiation that is not present in NLO QCD calculations could give an effective P_T smearing that affects the low P_T observed cross section. The second possible cause of the shape difference is the *bremsstrahlung* process [10], in which an initial or final state quark radiates a photon. QCD predictions show good agreement with recent measurements of this process at LEP [11], however a recent higher order calculation of this process [12] in $p\bar{p}$ collisions does indicate a prediction that is 5% steeper at $P_T = 16$ GeV/c. Finally, the differences could indicate that

for the first time we are measuring the gluon distribution inside the proton in a fractional momentum range where it has not been measured well before.

We thank the technical staffs of the participating institutions for their vital contributions. This work was supported by the DOE and NSF from the U.S., INFN of Italy, MESFC of Japan, and the A.P. Sloan Foundation. We also wish to thank J. F. Owens for providing his computer code for the theoretical calculations.

References

- [1] J. Owens. *Reviews of Modern Physics*, 59:465, 1987.
- [2] F. Abe *et al.* (CDF Collaboration). *Physical Review*, D(48):2998, 1993.
F. Abe *et al.* (CDF Collaboration). *Physical Review Letters*, 68:2734, 1992.
- [3] F. Abe *et al.* (CDF Collaboration). *Nuclear Instruments and Methods*, A(271):387, 1988.
- [4] The event z vertex cut was relaxed to $|z| < 60$ cm, and the missing transverse energy was required to be less than 80% of the photon transverse energy to remove cosmic rays.
- [5] Y.S. Tsai. *Rev. Mod. Phys.*, 46:815, 1974.
- [6] R. Brun *et al.* *GEANT3*. CERN DD/EE/84-1.
- [7] J. Ohnemus, H. Baer and J.F. Owens. *Physical Review*, D(42):61, 1990.
- [8] J. Botts *et al.* (CTEQ Collaboration). *Physics Letters*, B(304):159, 1993.

- [9] A.D. Martin, W.J. Stirling, and R.G. Robert. *Physics Letters*, B(306):145, 1993.
- [10] Edmond L. Berger and Jianwei Qiu. *Physical Review*, D(44):2002, 1991.
P. Aurenche *et al.* *Nuclear Physics*, B(33):34, 1993.
- [11] P.D. Acton *et al.* (OPAL Collaboration). *Zeitschrift fur Physik*, C(54):193, 1992 and references therein.
- [12] M. Gluck *et al.* *High- p_T Photon Production at $p\bar{p}$ Colliders*, Feb. 1994. DO-TH 94/02.

P_T Bin (GeV/c)	P_T (GeV/c)	# Events	# Photons	$d^2\sigma/dP_Td\eta$ (pb/(GeV/c))	Stat. (%)	Sys. (%)
10 – 16	12.3	3982	897	4.46×10^3	9.3	16
16 – 18	17.0	30046	13943	1.30×10^3	2.9	12
18 – 20	19.0	28165	14675	8.05×10^2	2.6	11
20 – 22	21.0	17427	9064	4.58×10^2	3.3	10
22 – 24	23.0	10923	6033	3.08×10^2	3.8	10
24 – 26	25.0	7042	4362	2.26×10^2	4.3	10
26 – 28	27.0	4642	3118	1.63×10^2	4.9	10
28 – 30	29.0	3169	2012	1.06×10^2	6.1	10
30 – 32	31.0	2240	1433	7.67×10^1	7.2	9
32 – 36	33.9	2883	1974	5.37×10^1	6.0	9
36 – 40	37.9	1548	1110	3.09×10^1	7.9	9
40 – 44	41.9	942	722	2.05×10^1	9.5	9
44 – 55	48.9	1135	710	7.61×10^0	10.0	10
55 – 72	62.4	659	564	3.09×10^0	10.2	10
72 – 92	80.8	205	184	9.11×10^{-1}	17.4	10
92 – 152	114.7	95	90	1.63×10^{-1}	25.2	11

Table 1: The cross section calculated using the profile and conversion methods is tabulated along with the statistical and systematic uncertainties. The systematic uncertainties include normalization uncertainties and are $\approx 100\%$ correlated bin to bin.

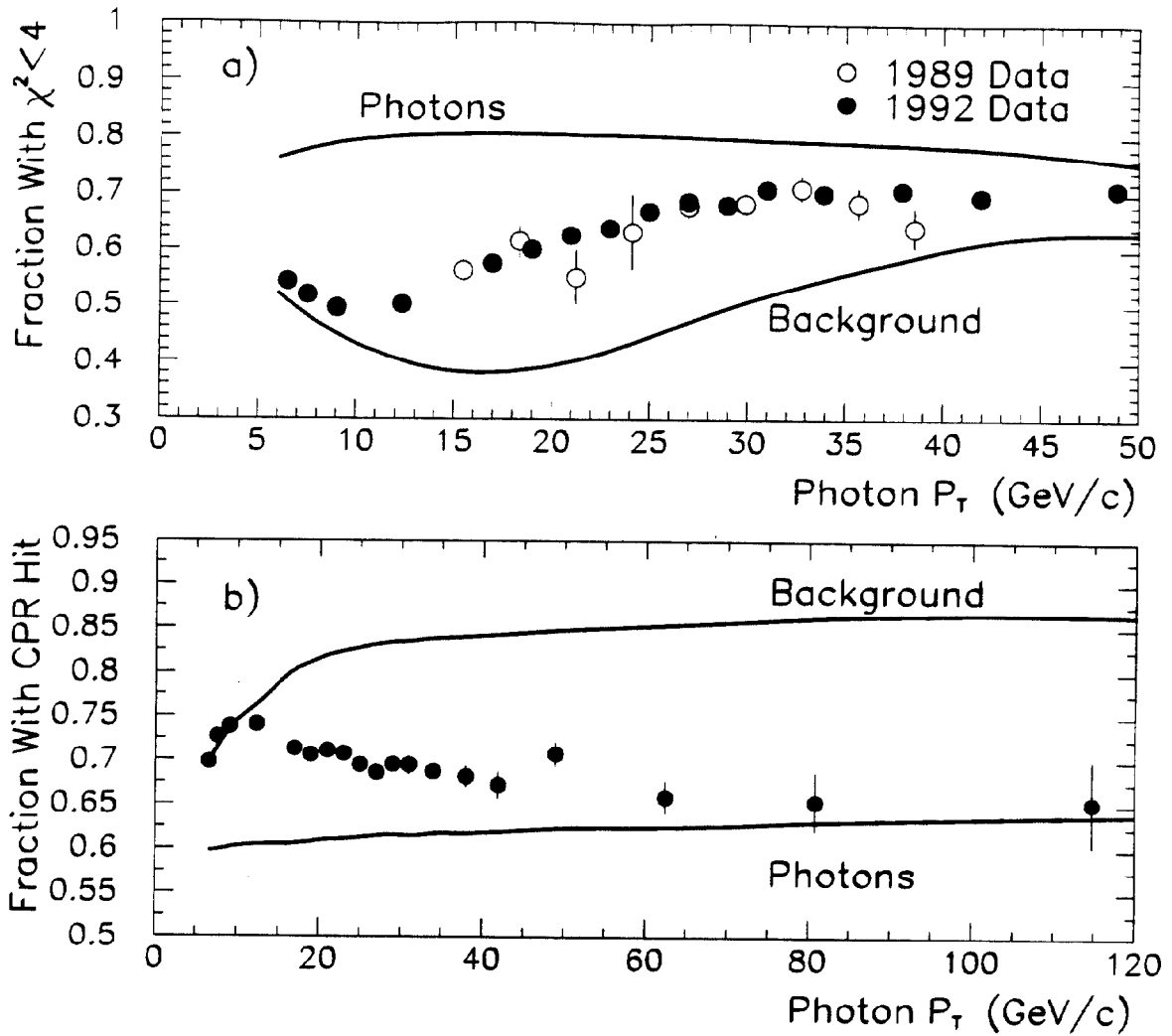


Figure 1: Illustration of the photon background subtraction methods. In a) is shown the profile method, with the fraction of photon candidates with $\chi^2 < 4$ (ϵ) along with the predictions for single photons (ϵ_γ) and background (ϵ_b). In b) the same is shown for the conversion method, with ϵ in this case being the fraction of photon candidates with a CPR signal.

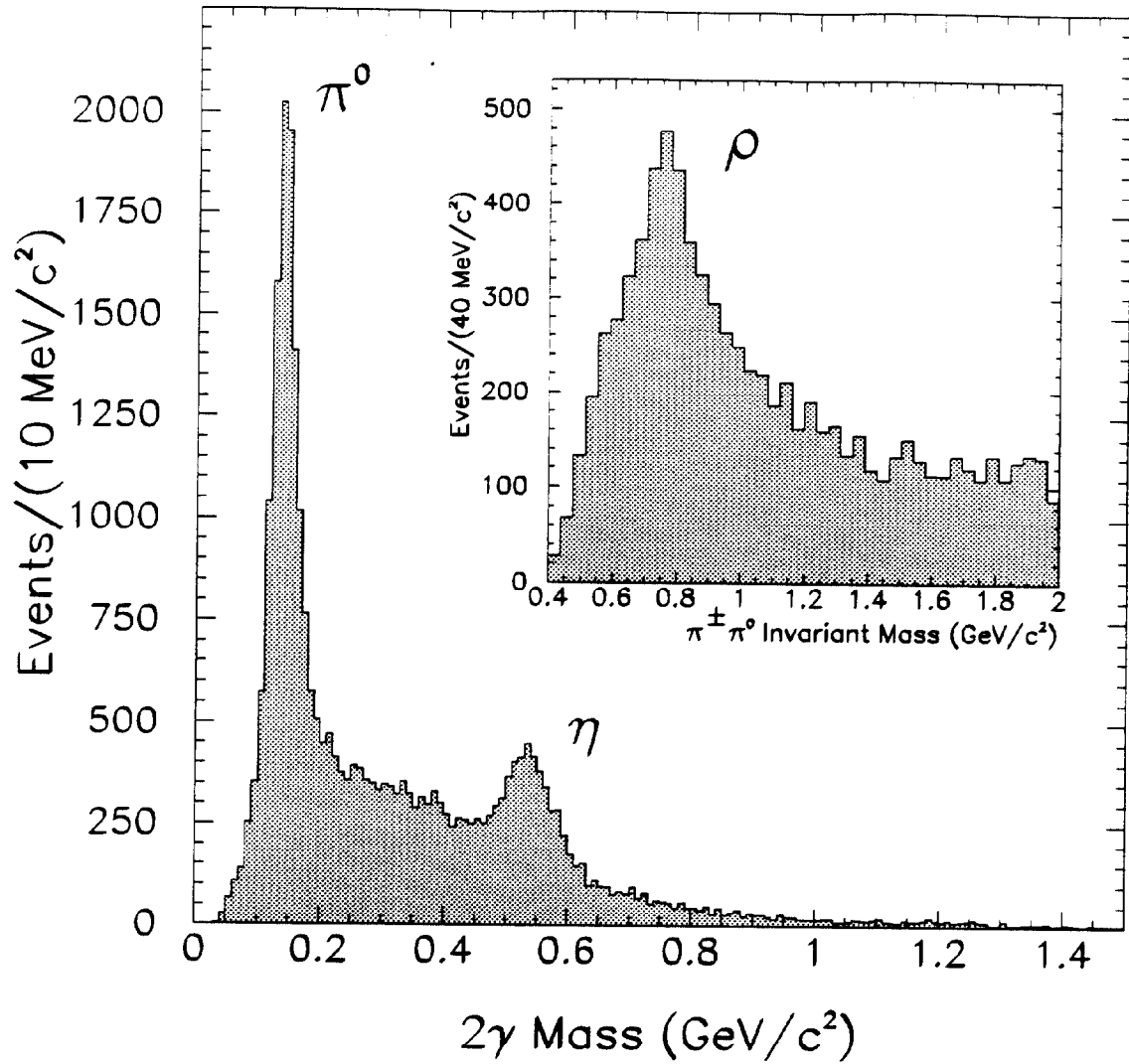


Figure 2: The 2 photon mass distribution, displaying reconstructed π^0 and η mesons. Inset is the reconstructed charged ρ meson peak. All three reconstructed mesons are used for the determination of the CPR conversion rate uncertainties.

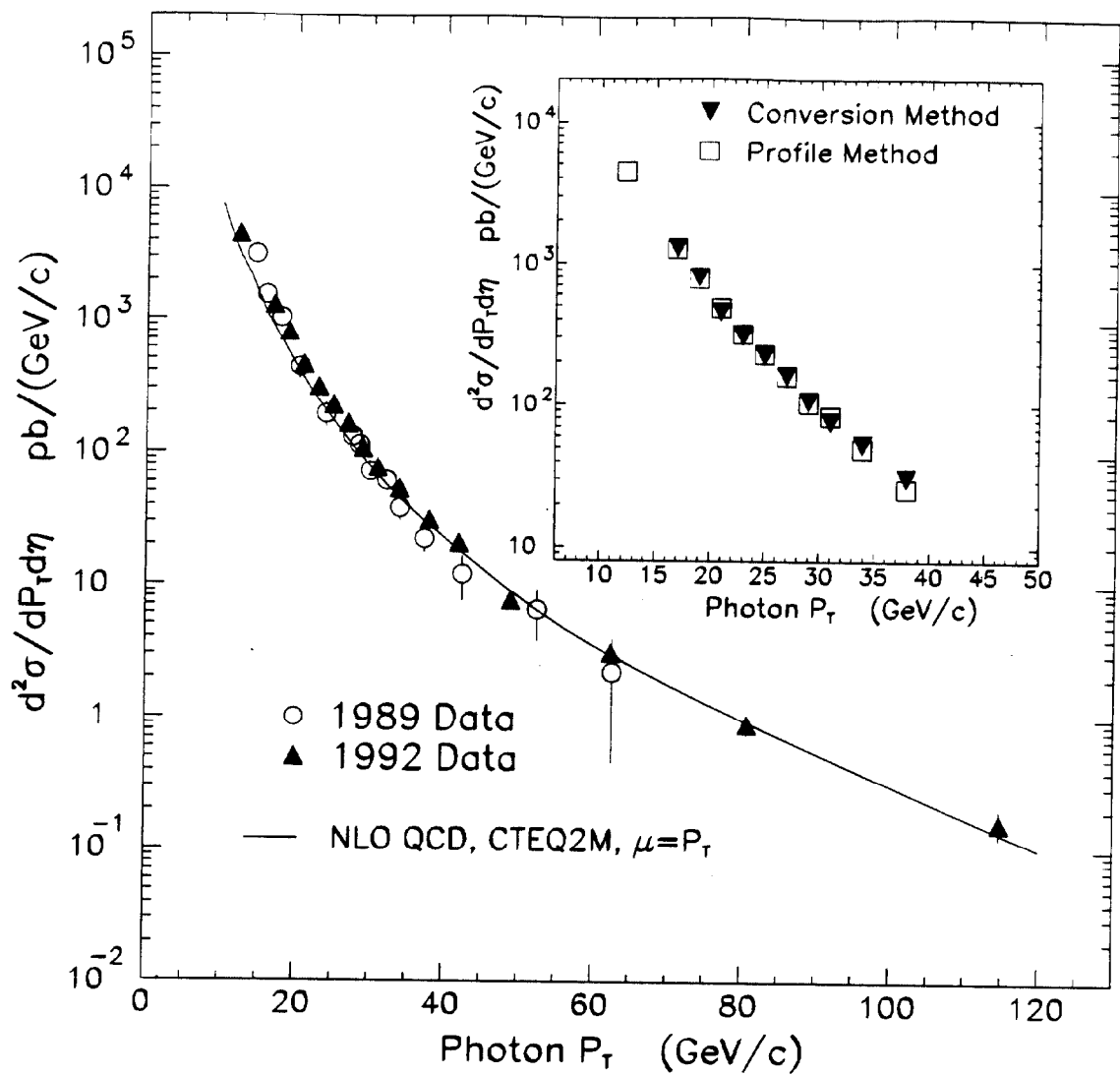


Figure 3: The inclusive isolated prompt photon cross section from 1989 and 1992 compared with a next-to-leading order QCD prediction. Inset is the comparison of the two background subtraction methods in their region of overlap.

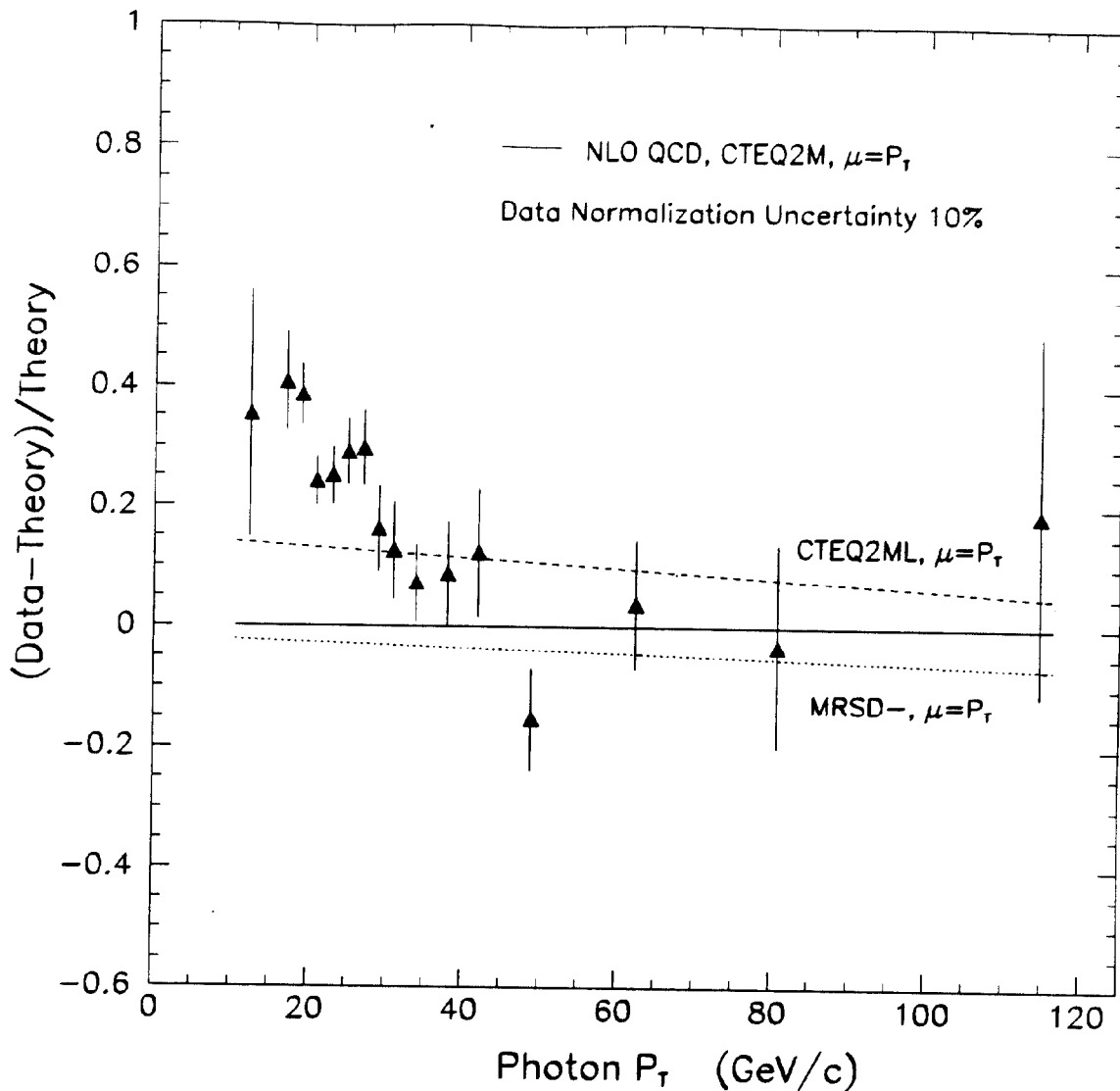


Figure 4: The prompt photon cross section measurement is compared with NLO QCD predictions and variations of parton distributions. The data has an additional 10% systematic uncertainty, which is nearly 100% correlated point-to-point and includes normalization uncertainties.